

Immobilized vanadium amino acid Schiff base complex on Al-MCM-41 as catalyst for the epoxidation of allyl alcohols

Elham Zamanifar · Faezeh Farzaneh

Received: 9 March 2011 / Accepted: 5 June 2011 / Published online: 24 June 2011
© Akadémiai Kiadó, Budapest, Hungary 2011

Abstract Vanadium complexes of *N*-salicylidene-L-histidine immobilized on Al-MCM-41 designated as VO(Sal-His)/Al-MCM-41, were prepared and characterized by X-ray powder diffraction (XRD), FT-IR, nitrogen adsorption–desorption and chemical analysis techniques. VO(Sal-His)/Al-MCM-41 was found to catalyze the epoxidation of *trans*-2-hexen-1-ol, cinnamyl alcohol and geraniol with *tert*-butyl hydroperoxide (TBHP). The successful catalytic behavior of VO(Sal-His)/Al-MCM-41 with 99% conversion and excellent selectivity toward the corresponding epoxides is described herein.

Keywords Al-MCM-41 · Vanadium complex · Epoxidation · Allyl alcohols

Introduction

The oxidation of organic substrates is potentially very useful, but is usually difficult to control. Significant research efforts have focused on the applicability of oxidation reactions by increasing their selectivity [1]. Despite impressive progress in the level of understanding of such reactions, which has led to various industrial applications [2], their practical use is still quite limited. In attempts to borrow know-how from nature, the study of so-called “biomimetic” or “bioinspired” reagents is enjoying increasing popularity [3, 4]. The goal of these reagents is to mimic the high activity and selectivity of enzymes in designing simpler models of their active sites. Many natural oxidizers contain one or more transition metals in the active center; prominent examples are the cytochrome P450 family [5], copper-based metalloproteins [6, 7], and vanadium-dependent haloperoxidases, which are one of the

E. Zamanifar · F. Farzaneh (✉)

Department of Chemistry, University of Alzahra, P.O. Box 1993891176, Vanak, Tehran, Iran
e-mail: faezeh_farzaneh@yahoo.com; farzaneh@alzahra.ac.ir

principle areas of the bioinorganic chemistry of vanadium [8–10]. The haloperoxides themselves catalyze a variety of oxidation reactions, such as the oxidation of bromide to hypobromite, the transformation of organic sulfides to sulfoxides, or the epoxidation of olefins, using different oxygen sources, such as air, hydrogen peroxide and other oxygen donors [11]. These transformations are particularly attractive from a synthetic point of view if the stereo control typical for enzymatic reactions can be fully exploited. In an attempt to gain insight into the biological roles of vanadium, many recent studies have focused on the coordination chemistry of this metal in the oxidation states of III, IV and V with biologically relevant ligands bearing oxygen and nitrogen atoms [12].

In the last decade, Schiff base ligands have received much attention, mainly because of their extensive application in the fields of synthesis and catalysis [13]. This attention is still growing; a considerable research effort is devoted to the synthesis of modified and supported reagents for catalysis and materials chemistry [14–16]. The Schiff bases of vanadium complexes are efficient catalysts for oxidation reactions both in homogeneous [17–26] and heterogeneous [27–30] systems. The activity of these complexes varies with the type of ligands, coordination sites and type of support in the heterogeneous catalysts.

Microporous and mesoporous materials that encapsulate metal complexes hold a key place as model compounds for mimicking enzymes. In fact, these supports act as the protein portion of a natural enzyme in the model and also offer the advantages of easy recovery and catalyst reuse.

In continuation of our research on vanadium catalyzed epoxidation reactions [31], herein, we report the effect of immobilized tridentate *N*-salicylidene-L-histidine Schiff base vanadium complex within the nanoreactors of Al-MCM-41 as catalysts for the epoxidation of geraniol, cinnamyl alcohol and *trans*-2-hexene-1-ol.

Experimental

All materials were of commercial reagent grade and used without further purification. TBHP (80% in di-*tert*-butyl peroxide), was purchased from Fluka, vanadyl sulfate and geraniol were obtained from Aldrich. Methyl amine, cetyltrimethylammonium bromide (CTABr), tetraethylorthosilicate (TEOS), aluminum hydroxide, salicylaldehyde, L-histidine, sodium acetate, chloroform, *trans*-2-hexen-1-ol, cinnamyl alcohol, acetone, commercial reagent grade diethyl ether and ethanol were purchased from Merck Chemical Company. FT-IR spectra were recorded on a Bruker Tensor 27 FT-IR Spectrometer using KBr pellets over the range of 4000–400 cm^{−1}. The UV–Vis measurements were performed on a double beam UV–Vis Perkin Elmer Lambda 35 spectrophotometer. X-ray powder diffraction (XRD) data were recorded on a diffractometer type, Seifert XRD 3003 PTS, using Cu K_{α1} radiation ($\lambda = 1.5406 \text{ \AA}$). Chemical analysis of samples was carried out with a Perkin-Elmer atomic absorption spectrometer (AAS). Nitrogen sorption studies were performed at liquid nitrogen temperature (77 K) using a Quanta chrome Nova Win 2, version 2.2. Before the adsorption experiments, the samples were out-gassed under nitrogen gas during 7 h at 423 K. TGA/DTA were carried

out by Mettler-Toledo TGA/s-DTA-851. Oxidation products were analyzed by GC and GC-MS using an Agilent 6890 Series with a FID detector, HP-5, 5% phenylmethyl siloxane capillary and an Agilent 5973 Network, mass selective detector, HP-5 MS 6989 Network GC system.

Synthesis of Al-MCM-41

The Al-MCM-41 (Si/Al = 50) was prepared according to a previously reported method [32]. Methylamine (2.08 mL) was added to deionized water (42 mL) and the mixture was stirred at room temperature for 10 min. CTABr (1.47 g) was then added and the mixture was stirred for another 60 min until a clear solution formed. Then, a TEOS solution (2.1 mL) was added dropwise to the solution followed by addition of aluminum hydroxide solution (0.03 g in 5 mL deionized water). The molar composition of the resulting mixture was SiO₂: 1.6 MA: 0.215 CTMABr: 125 H₂O: 0.02 Al₂O₃. The pH of the reaction mixture was adjusted to 8.5 by the slow addition of a hydrochloric acid solution (1 M). After slow stirring for 2 h, the solid was separated by centrifugation and washed with methanol. Al-MCM-41 was obtained as a white powder after drying the solid at 45 °C for 12 h followed by calcination at 550 °C for 8 h to decompose the surfactant.

Preparation of [VO(Sal-His)(H₂O)]·3H₂O

[VO(Sal-His)(H₂O)]·3H₂O was prepared according to a procedure described previously [19]. Salicylaldehyde (10 mmol) in ethanol (20 mL) was introduced into a histidine solution (10 mmol) dissolved in water (20 mL), followed by the addition of an aqueous sodium acetate solution (0.02 mol in 10 ml water). The color of the solution changed to deep yellow after this addition. An aqueous solution of VOSO₄·3H₂O (8 mmol in 10 mL water) was then added slowly to the mixture while stirring. The resulting solution, whose color changed from deep yellow to dark red, was concentrated slowly with a rotary evaporator. The solid was filtered, washed with a large amount of water, acetone, and diethyl ether, then dissolved in ethanol (20 mL), followed by the addition of water (50 mL). The mixture was slowly concentrated with a rotary evaporator to obtain the complex compound.

Anal. Calc.: for C₁₃H₁₅N₃O₅V·3H₂O ($M = 395 \text{ gmol}^{-1}$): V 12.91, C 39.49, H 4.56, N 10.63. Found: V 12.92, C 39.75, H 4.49, N 10.58%. FT-IR(cm⁻¹): 3143–3024(OH), 1629(C=N or COO), 1545(C=C), 1470, 1339, 1297(O-Ph), 941(V=O), which are consistent spectral bands with those reported previously [32]. UV-Vis: λ_{\max} at 251, 269, 358, 479 nm [33].

Preparation of catalyst

Al-MCM-41 (1 g) was added to the complex (0.25 mmol in 20 mL ethanol). The mixture was refluxed while stirring for 8 h. The solids were filtered, washed with hot ethanol and the resultant VO(Sal-His)/Al-MCM-41 was dried in air at room temperature. The percentage of vanadium present determined by AAS was 0.25%.

Catalytic epoxidation, general procedure

All epoxidation reactions of the allyl alcohol (geraniol, cinnamyl alcohol and *trans*-2-hexen-1-ol) were carried out in a round bottom flask equipped with a stir bar and a water-cooled condenser under atmospheric pressure. Typically, a mixture of catalyst (100 mg) and substrate (20 mmol, dissolved in 10 mL chloroform) was added to the reaction flask upon slow stirring. After a few minutes, TBHP (24 mmol, 80% in tertiary butyl peroxide) was added and the mixture was refluxed for 8 h. The solid was then filtered and washed with fresh chloroform. The filtrate was subjected to GC and GC mass analysis.

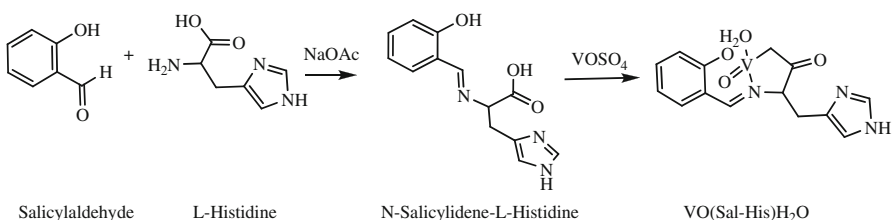
Results and discussion

The Schiff base ligand was prepared via condensation of salicylaldehyde and histidine, followed by treatment of the prepared ligand with $\text{VO}(\text{SO}_4)$ under aerobic conditions to give the desired oxovanadium complex (Scheme 1). The FT-IR, UV-Vis and CHN analysis were consistent with those of the authentic sample reported previously [33].

Fig. 1a shows the X-ray powder diffraction pattern of calcined Al-MCM-41, which exhibits one strong and one weak peak. All two XRD reflections were consistent with those previously reported [31] and can be indexed on a hexagonal lattice. The XRD patterns of $\text{VO}(\text{Sal-His})/\text{Al-MCM-41}$, shown in Fig. 1b, display a decrease in the peak intensities compared to the calcined Al-MCM-41 peaks. This change indicates that the Al-MCM-41 pore and surface silanol groups reacted with the vanadium complexes.

The N_2 adsorption–desorption isotherms of Al-MCM-41 and $\text{VO}(\text{Sal-His})/\text{Al-MCM-41}$ are shown in Fig. 2. The type IV isotherms [34] indicate that adsorption takes place as a thin layer on the walls at low relative pressures, P/P_0 (monolayer coverage). In addition, the inflection heights of $\text{VO}(\text{Sal-His})/\text{Al-MCM-41}$ in the nitrogen adsorption isotherm plots are smaller than those of Al-MCM-41. This phenomenon is attributed to the reduced pore volume that decreases from 1.074 to $0.8862 \text{ cm}^3 \text{ g}^{-1}$, which reflects the decrease in surface area (Table 1). This effect can be due to the inclusion of $\text{VO}(\text{Sal-His})$ on the Al-MCM-41.

The FT-IR spectra of $\text{VO}(\text{Sal-His})$, $\text{VO}(\text{Sal-His})/\text{Al-MCM-41}$, Al-MCM-41 and the subtracted spectrum of the immobilized complex within Al-MCM-41 from that



Scheme 1

Fig. 1 XRD of *a* calcined Al-MCM-41 and *b* VO(Sal-His)/Al-MCM-41

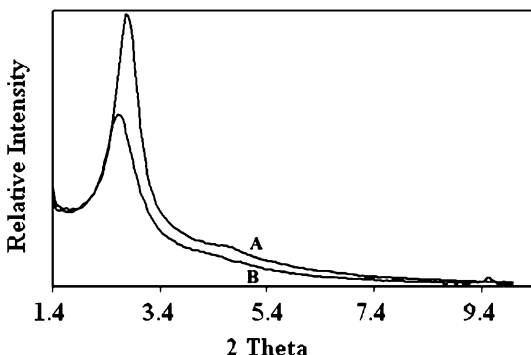


Fig. 2 Nitrogen adsorption–desorption isotherms *a* Al-MCM-41 and *b* VO(Sal-His)/Al-MCM-41

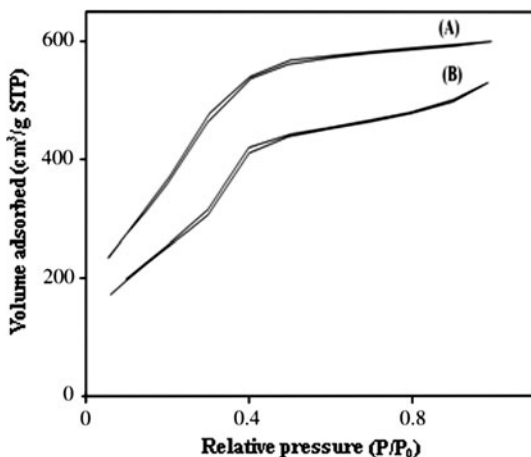


Table 1 Texture parameters of samples taken from XRD and nitrogen sorption studies

Material	XRD d Value (Å)	Lattice parameter (Å)	BET ^a ($\text{m}^2 \text{ g}^{-1}$)	Pore volume ($\text{cm}^3 \text{ g}^{-1}$)	Average pore diameter (Å)
Al-MCM-41	32.5	37.53	1455	1.0740	20.72
VO(Sal-His)/Al-MCM-41	34.3	39.61	981.5	0.8862	19.32

^a Specific surface area

of Al-MCM-41 are shown in Fig. 3a, b, c, d and in Table 2. The broad bands appearing from 3424 to 3401 cm^{-1} may be attributed to the surface silanol and –OH groups of adsorbed water. After the immobilization of the complex within Al-MCM-41 some weak peaks appear at the region 2987–2900 cm^{-1} due to the C–H and N–H vibrations of the immobilized complex. The bands at 1222, 1219, 1141 and 1133 cm^{-1} are due to the asymmetric stretching vibrations of Si–O–Si bridges, and those appear at 967–950 cm^{-1} arise from Si–O–Al, VO–Si and V=O stretching vibrations. However, the band due to the V=O stretching vibration, which appears at 970 cm^{-1} in the free complex could not be observed probably because it

Fig. 3 FT-IR spectra of *a* VO(Sal-His), *b* VO(Sal-His)/Al-MCM-41, *c* Al-MCM-41, and *d* the spectrum of the difference of VO(Sal-His)/Al-MCM-41 and Al-MCM-41

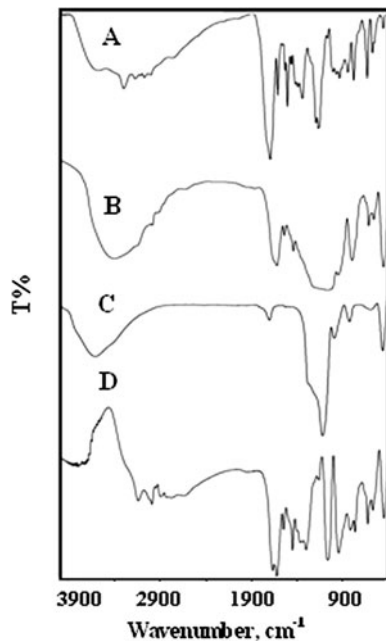


Table 2 IR band assignment corresponding wavenumbers (cm^{-1}) obtained for Al-MCM-41 and immobilized vanadium complex within nanoreactors of Al-MCM-41

Catalyst	(Si–OH)	(Si–O–Si) _{asym}	(Si–OAl)/(Si–V) _{asy}	(Si–O–Si) _s	C=N
Al-MCM-41	3424	1082, 1219	961	803	—
VO(Sal-His)/Al-MCM-41	3401	1080, 1222	956	804	1672
[VO(Sal-His) (H ₂ O)]·3H ₂ O	—	—	—	—	1623

is masked by the strong and broad Si–O–Si and Si–O–Al vibration positioned at 1200–950 cm^{-1} . The C=N stretching frequency of the immobilized vanadium complex within the Al-MCM-41 appears at 1672 cm^{-1} [35, 36].

TGA/DTA patterns of VO(Sal-His)/Al-MCM-41 are shown in Fig. 4. The weight loss of the complex immobilized within nanoreactors of Al-MCM-41 takes places at two steps. The first weight loss of 1% is observed below 200 °C, corresponding to the evaporation of water. The second weight loss observed at about 200–550 °C is due to the decomposition of the organic ligand, consistently with DTA results.

Epoxidation of alkenes catalyzed by VO(Sal-His)/Al-MCM-41

The epoxidation reactions were carried out in the presence of 0.1 g of the VO(Sal-His)/Al-MCM-41 as catalyst at different times using geraniol as the representing substrate in order to choose the best reaction time. The results are presented in Fig. 5. As seen, geraniol is mostly oxidized after 4 h, beyond which no considerable oxidation occurs during the next 4 h.

Epoxidation results obtained for geraniol, cinnamyl alcohol and *trans*-2-hexen-1-ol using TBHP in chloroform in the presence of VO(Sal-His)/Al-MCM-41 are given in Scheme 2 and Tables 3, 4, and 5. The identification of the products was carried out by

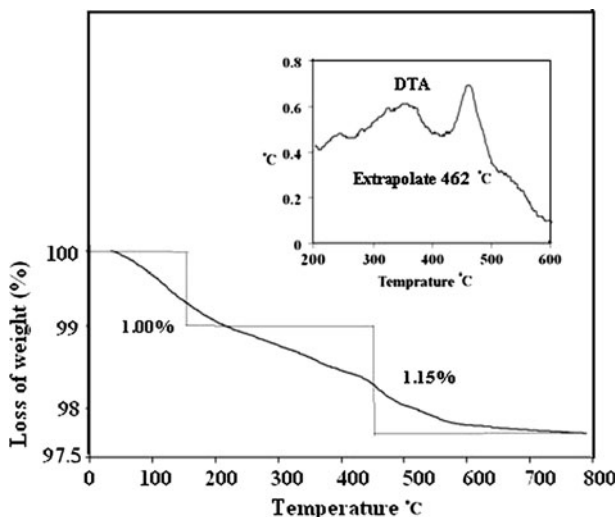
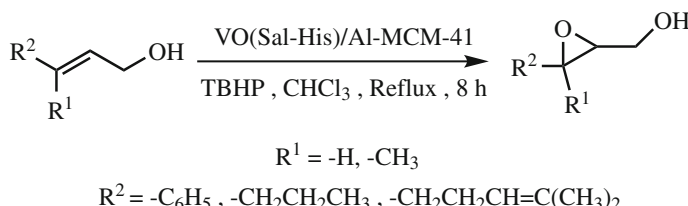
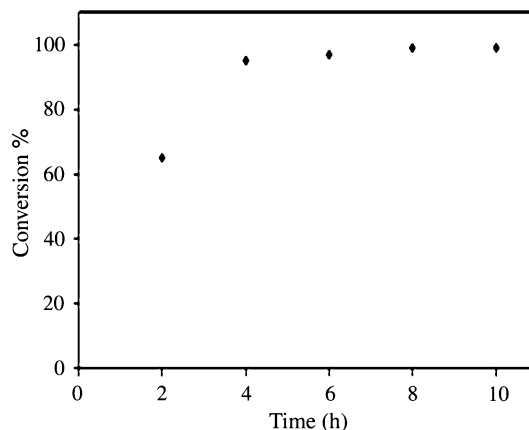


Fig. 4 TGA VO(Sal-His)/Al-MCM-41, inset is DTA of the same compound

Fig. 5 Conversion of geraniol at different times in the presence of VO(Sal-His)/Al-MCM-41 catalyst



Scheme 2

Table 3 Results of catalytic epoxidation of geraniol with TBHP in the presence of catalysts

Entry	Catalyst	Conversion (%)	Selectivity (%)	TON			
				Geraniol	2,3-Epoxygeraniol	Others ^a	TON
1	VO(Sal-His)/Al-MCM-41	99	99	—	—	—	4040
2	VO(Sal-His)/Al-MCM-41 ^b	95	63	29	29	8	3877
3	VO/AlMCM41	27	77	13	13	10	3375
4	[VO(Sal-His) (H ₂ O) ₃ H ₂ O] ^c	48	60	31	31	9	980
5	Al-MCM-41	10	—	91	91	9	9

Reaction conditions: Catalyst (0.1 g), substrate (20 mmol), TBHP (24 mmol), solvent (chloroform, 10 mL, under reflux), time (8 h); TON is the mmol of product to mmol vanadium present in catalysts

^a Others are linalool oxide and pulegone

^b The reaction was carried out in the presence of recovered catalyst

^c The reaction was carried out in the presence of homogeneous catalyst

Table 4 Results of catalytic epoxidation of cinnamyl alcohol with TBHP in the presence of catalysts

Entry	Catalyst	Conversion (%)	Selectivity (%)	TON ^a				
				Cinnamyl alcohol	(3-phenyloxiran-2-yl)methanol	Benzaldehyde	Cinnamaldehyde	Others
1	VO(Sal-His)/Al-MCM-41	90	90	5	58	23	4	3
2	VO-Al-MCM-41 ^b	25	15	58	4	23	4	3

Reaction conditions: similar to Table 3

^a TON is the mmol of product to mmol vanadium present in catalysts^b Catalyst leaching was observed

Table 5 Results of catalytic epoxidation of *trans*-2-hexene-1-ol with TBHP in the presence of catalysts

Entry	Catalyst	Conversion (%)	Selectivity (%)	TON ^a
1	VO(Sal-His)/Al-MCM-41	60	100	2449
2	VO-Al-MCM-41	32	100	4000

Reaction conditions: similar to Table 3

^a TON is the mmol of product to mmol vanadium present in catalyst

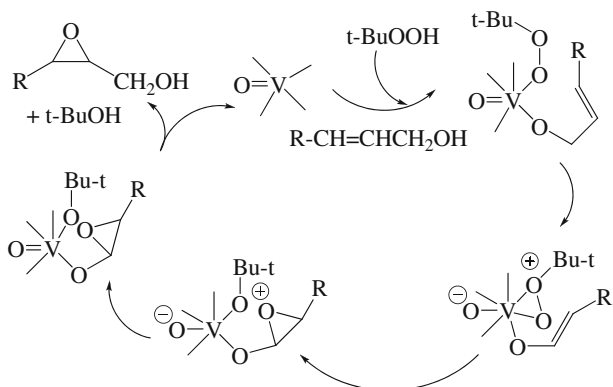
comparing the mass spectra with those of the authentic samples. We have included the effect of recovered VO(Sal-His)/Al-MCM-41, VO-Al-MCM-41, Al-MCM-41 void of complexes as catalysts and [VO(Sal-His)H₂O]·3H₂O as a homogeneous catalysis system in Table 3 in order to make the comparisons more convenient.

As seen in Table 3, geraniol is almost quantitatively oxidized to 2,3-epoxygeraniol in the presence of VO(Sal-His)/Al-MCM-41 (Table 3, entry 1) with 99% conversion and 99% selectivity towards the corresponding epoxides. Catalytic efficiencies are observed using recovered VO(Sal-His)/Al-MCM-41 (Table 3, entry 2), VO-Al-MCM-41 (Table 3, entry 3), [VO(Sal-His)H₂O]3H₂O (Table 3, entry 4), Al-MCM-41 (Table 3, entry 5). Therefore, the key roles of the vanadium complex as well as the heterogeneous character of the catalyst are evidenced (Fig. 5).

The maximum amount of cinnamyl alcohol conversion and selectivity toward the formation of 3-phenyl-oxiran-2-yl methanol occurs in the presence of VO(Sal-His)/Al-MCM-41 as the oxidation catalyst (Table 4, entry 1). Epoxidation reactions proceed less efficiently under VO-Al-MCM-41 (Table 4, entry 2). Therefore, both the presence of the coordinated Schiff base ligand as well as the heterogeneous catalytic character of the system drastically enhances the cinnamyl alcohol conversion percentage and selectivity toward the formation of the corresponding epoxide.

The epoxidation results of *trans*-2-hexen-1-ol to 2, 3-epoxyhexanol with VO(Sal-His)/Al-MCM-41 as catalysts are presented in Table 5. Compared to geraniol and cinnamyl alcohol, the epoxidation reaction of *trans*-2-hexen-1-ol proceeds less efficiently, but with 100% selectivity to the corresponding epoxide. Utilization of VO-Al-MCM-41 as catalysts decreases the conversion rate from 60 to 32%.

The increasing reactivity trend of geraniol > cinnamyl alcohol > *trans*-2-hexen-1-ol observed in our reactions may be used as a criterion in gaining insight into the reaction mechanism. This trend reveals that the highly substituted allyl alcohol exhibits the highest epoxidation reactivity. Such observations are reminiscent of the mechanism suggested by Sharpless for the vanadium-catalyzed epoxidations in which the more highly substituted alkenes react faster than the less substituted alkenes [26]. According to this mechanism, both the allylic alcohol and the hydroperoxide initially coordinate to the metal center. Subsequent coordination of the second oxygen of the peroxide generates metal peroxide. Displacement of the epoxide probably proceeds with the loss of the *tert*-butoxy ligand to regenerate the vanadium catalyst (Scheme 3).

**Scheme 3**

The stability of the VO(Sal-His)/Al-MCM-41 was also studied by recycling the recovered catalyst and through the determination of the metal content using atomic absorption spectroscopy. The vanadium content was shown to be 0.245% with very little change (0.005%,) with respect to the initial catalyst vanadium content (0.25%). As shown in Table 3, entry 2, the recovered VO(Sal-His)/Al-MCM-41 catalyzed the epoxidation of geraniol with a minor decrease in conversion and TON (no. of moles of products/no. of moles of vanadium complex), although with lower selectivity toward the formation of the corresponding epoxide.

The last worthwhile point to emphasize is the highly heterogeneous character of the VO(Sal-His)/Al-MCM-41 catalysts used in this work. The experimental evidence ruled out the effect of the participation of any leaching active species from the solid catalysts in the epoxidation reactions.

Epoxidation of allyl alcohols especially geraniol has been studied previously with homogeneous and heterogeneous catalysts, amongst which VO(acac)₂ has proven to be the most active catalysis system. Recently, anchoring of vanadylacetetylacetone onto amine-functionalized clays [37] and mesoporous HMS [38] has been used for the epoxidation of geraniol with high activity and selectivity. On the other hand, immobilization of the catalyst within HMS rather than grafting has provided lower activity with some leaching [38]. We have studied a new Schiff base complex of vanadium VO(Sal-His) immobilized within Al-MCM-4 as catalyst for epoxidation of allyl alcohols, especially geraniol in this work. Observation of high activity and selectivity, stability and reusability of the catalyst with no leaching during the course of reactions is promising.

Conclusions

The vanadium complex [VO(Sal-His)(H₂O)]·3H₂O immobilized within the nanoreactors of Al-MCM-41 was prepared and characterized. It was found that VO(Sal-His)/Al-MCM-41 successfully catalyzes the epoxidation of *trans*-2-hexene-1ol, cinnamyl

alcohol and geraniol with 60–99% conversion and excellent selectivity. Therefore, mesoporous materials with a larger amount of room, such as Al-MCM-41, accommodate both the oxidant and substrates with different sizes in approaching the catalytically active metal centers. The observation of such catalytic behavior with no significant amount of catalyst desorption during the course of the studied reactions as well as almost quantitative epoxidation of geraniol in this study merits consideration by specialists.

Acknowledgments The financial support from the University of Alzahra is gratefully acknowledged.

References

1. Shilov AE, Shulpin GB (1997) *Chem Rev* 97:2879–2932
2. Bregeault JM (2003) *Dalton Trans*: 3289–3302
3. Gamez P, Aubel PG, Driessens WL, Reedijk J (2001) *Chem Soc Rev* 30:376–385
4. Lightenbarg AGJ, Hage R, Feringa BL (2003) *Coord Chem Rev* 237:89–101
5. Ortiz de Montellano PR (ed) (1995) Cytochrome P450: structure, mechanisms and biochemistry, 2nd edn. Plenum Press, New York
6. Klinmann JP (1996) *Chem Rev* 96:2541–2561
7. Solomon EI, Sundaram UM, Machonkin TE (1996) *Chem Rev* 96:2563–2606
8. Rehder D (2008) Bioinorganic vanadium chemistry. John wiley sons & Ltd Press, Chichester, pp 105–128
9. Rehder D (2003) *Inorg Chem Commun* 6:604–617
10. Thomson KH, Mcneill JH, Orvige C (1999) *Chem Rev* 99:2561–2571
11. Dembitsky VM (2003) *Tetrahedron* 59:4701–4720
12. Rehder D (2008) Bioinorganic vanadium chemistry. John wiley & sons Ltd, Chichester, pp 13–53
13. Canali L, Sherrington DC (1999) *Chem Soc Rev* 28:85–93
14. Kojima M, Taguchi H, Tsuchimoto M, Nakajima K (2003) *Coord Chem Rev* 237:183–196
15. Lane BS, Burgess K (2003) *Chem Rev* 103:2457–2473
16. Gupta KC, Sutar AK (2008) *Coord Chem Rev* 252:1420–1450
17. Boghaei DM, Mohebi S (2002) *J Mol Catal A* 179:41–51
18. Kwiatkowski E, Romanowski G, Nowicki W, Kwiatkowski M, Suwinska K (2003) *Polyhedron* 22:1009–1018
19. Ando R, Inden H, Sugino M, Ono H, Sakaeda D, Yagyu T, Maeda M (2004) *Inorg Chim Acta* 357:1337–1344
20. Kwiatkowski E, Romanowski G, Nowicki W, Kwiatkowski M, Suwinska K (2007) *Polyhedron* 26:2559–2568
21. Rayati S, Sadeghzadeh N, Khavasi HR (2007) *Inorg Chem Commun* 10:1545–1548
22. Romanowski G, Kwiatkowski E, Nowicki W, Kwiatkowski M, Lis T (2008) *Polyhedron* 27: 1601–1609
23. Rayati S, Koliae M, Ashouri F, Mohebbi S, Wojtczak A, Kozakiewicz A (2008) *Appl Catal A* 346:65–71
24. Cordelle C, Agustin D, Daran JC, Poli R (2010) *Inorg Chim Acta* 304:144–149
25. Yaul AR, Pethe GB, Aswar AS (2010) *Russ J Coord Chem* 36:254–258
26. Sharpless KB, Verhoven TR (1979) *Aldrichim Acta* 12:63–74
27. Maurya MR, Chandrakar AK, Chand S (2007) *J Mol Catal A* 270:225–235
28. Maurya MR, Chandrakar AK, Chand S (2007) *J Mol Catal A* 274:192–201
29. Gupta KC, Sutar AK, lin C (2009) *Coord Chem Rev* 253:1926–1946
30. Yang Y, Zhang Y, Hao S, Guan J, Ding H, Shang F, Qiu P, Kan Q (2010) *Appl Catal A* 381:274–281
31. Farzaneh F, Zamanifar E, Williams CD (2004) *J Mol Catal A* 218:203–209
32. Zanjanchi MA, Sh Asgari (2004) *Solid State Ionics* 171:277–282
33. Pessoa JC, Cavaco I, Correia I, Duarte MT, Gillard RD, Henriques RT, Higes FJ, Madeira C, Tomaz I (1999) *Inorg Chim Acta* 293:1–11
34. Lynch J (2001) Physico-chemical analysis of industrial catalysts. Technip ed., Paris

35. Selvaraj M, Pandurangan A, Seshadri KS, Sinha PK, Krishnasamy V, Lal KB (2003) *J Mol Catal A* 192:153–170
36. Kozlov A, Asakura K, Iwasawa Y (1998) *Micropor Mesopor Mater* 21:571–579
37. Pereira C, Silva AR, Carvalho AP, Pires J, Freire C (2008) *J Mol Catal A* 283:4–14
38. Jarrais B, Pereira C, Silva AR, Carvalho AP, Pires J, Freire C (2009) *Polyhedron* 28:994–1000